Bonding in ClF_n ($n = 1-7$) Molecules: Further Insight into the Electronic Structure of Hypervalent Molecules and Recoupled Pair Bonds†

Lina Chen,* David E. Woon,* and Thom H. Dunning, Jr.

Department of Chemistry, University of Illinois at Urbana−Champaign, Box 37-6, CLSL, 600 South Mathews, Urbana, Illinois 61801

Received: May 29, 2009; Revised Manuscript Received: July 9, 2009

As a result of new studies into the nature of hypervalent molecules, we identified a new type of bond called a *recoupled pair bond*. Hypervalency or hypercoordination was shown to arise by decoupling a pair of valence electrons, each of which becomes available to participate in a new bond. Energy must be expended to decouple an electron pair, so the first recoupled pair bond is weaker than the analogous covalent bond. However, the second bond, which involves a singly occupied antibonding orbital in the hypervalent fragment, is stronger than the analogous covalent bond. Following an initial study of SF_n species ($n = 1-6$), the present work explores the ClF_n ($n = 1-7$) series to further examine the explanatory usefulness of the recoupled pair bonding model. Optimized structures and energies of the ground and low-lying excited states of the ClF_n molecules were determined by employing high level *ab initio* calculations [MRCI, CCSD(T)] with correlation consistent basis sets. Low-lying states that are due to recoupled pair bonding are found in ClF ($^3\Pi$) and ClF_2 ($^2A_1$, $^2B_1$, $^2A'$, $^4A_2$). The bond energies for F addition to form ClF_2, ClF_4, and ClF_6 were found to be much lower than those leading to ClF, ClF_3, and ClF_5. The same type of oscillation is observed in SF_n species. The differences between ClF_n and SF_n reflect the fact that the $3s^2$ and $3p^2$ electron pairs are more strongly bound in Cl than in S. This behavior and other trends observed in the ClF_n species demonstrate the improved predictive ability of the recoupled pair bonding model over other models for describing hypervalent bonding.

I. Introduction

Debates on the nature of chemical bonding have been a recurring theme in the development of modern quantum chemistry. One of the areas of controversy has been the category of molecules where the central atoms could be viewed as possessing more than eight valence electrons, violating Lewis's octet rule. To explain the bonding in such molecules, Musher[1] proposed the concept of hypervalent bonding in 1969. In his definition (p 55), hypervalent molecules are those "...formed by elements in Groups V−VIII of periodic table in any of their valences other than their lowest stable chemical valence of 3, 2, 1, and 0 respectively." The related concept of hypercoordination was introduced by Schleyer in 1984.[2] Controversy over the extent of d orbital hybridization has been a subtheme in the study of hypervalency, but the issue has been resolved for some time.[3] Jensen[4] provides a brief historical summary of the work that led to the most widely accepted model for understanding the nature of hypervalency, the concept of three-center four-electron bonding (3c-4e), as proposed and developed by Rundle,[5] Pimentel,[6] and others.[7]

In the course of a previous study[8] on SF_n species from SF to SF_6, we developed a new model for understanding hypervalent behavior that offers more predictive capability than the (3c-4e) bonding model. We found that hypervalent bonding is distinctly different from typical covalent bonding. In contrast to the simple singlet coupling of electrons in singly occupied orbitals that occurs in covalent bonding, a pair of electrons in a nonbonding valence orbital must first be decoupled to form a hypervalent bond. Each of the two electrons can then be recoupled with an electron from another atom to form a chemical bond, so we call this *recoupled pair bonding*. Since the formation of this type of bond gives rise to hypercoordinated species, we equate recoupled pair bonding with hypervalent bonding.

The nature of the bonding in hypervalent species is best understood by studying successive additions of single atoms or radicals to the hypervalent atom. Examining the individual addition steps as well as the nature of the resulting bonds provides insights well beyond what can be found by merely studying hypervalent species near their equilibrium geometries (as previous work has done). For example, the dramatic variations in bond energies observed[9] in $SF_{n-1}-F$ bonds can be easily understood.[8] When a pair of electrons is recoupled through separate additions, the remaining electron occupies an antibonding orbital. If the antibonding orbital strongly overlaps with the bond pair, it both lengthens and weakens the recoupled pair bond.[10] However, when a second bond is formed, the effect of the antibonding orbital is decreased significantly, reducing the bond length of the first bond and yielding a second bond that is much stronger than the analogous normal covalent bond. From these and other observations, we have assembled a set of guidelines for understanding the formation of the ground and low-lying excited states of hypervalent species. The guidelines will be summarized in section III and then applied to the ClF_n series.

The rest of the paper is organized as follows. The computational methods are briefly described in section II. We then outline recoupled pair bonding guidelines and use them to predict possible stable structures of the ground states and some low-lying excited states of the ClF_n series. Results for ClF_n are presented in section IV and then briefly compared with the SF_n series in section V. We finally conclude in section VI with a brief discussion about future theoretical research.

† Part of the "Russell M. Pitzer Festschrift".

* Corresponding authors. E-mail: linachen@uiuc.edu (L.C.); dewoon@uiuc.edu (D.E.W.). Phone: +1-217-333-7748. Fax: +1-217-244-3186.

10.1021/jp905064v CCC: $40.75
Published on Web 08/12/2009

II. Methodology

Most of the *ab initio* calculations reported below were performed with the Molpro suite of programs[11] (version 2002.6). Standard coupled cluster calculations at the CCSD(T) or RCCSD(T)[12] level were carried out for the entire series of neutral ClF_n ($n = 1-7$) species, including their ground and low-lying excited electronic states. Subsequently, the optimized ground state energies of these species were used to determine the bond dissociation energies of $ClF_n \rightarrow ClF_{n-1} + F$ ($n = 1-7$). All valence electrons are correlated in the CCSD(T) or RCCSD(T) calculations.

Potential energy curves were computed around the minima of the states of ClF and ClF^+. For these species, multireference methods were also used to determine optimized energies and geometries and to examine the process of bond formation. Complete active space self-consistent field (CASSCF) wave functions[13] were used for this due to their ability to describe both covalent and hypervalent bond formation for all values of R_{ClF}. A nearly full valence CAS treatment was used: the 2s orbital of F was forced to be doubly occupied in all configurations. Degenerate configurations were state averaged for $ClF(^3\Pi)$. Subsequent multireference configuration interaction (MRCI) calculations[14] were performed to account for dynamical correlation. The Davidson correction[15] for quadruple excitations (MRCI+Q) was also included.

Augmented correlation consistent basis sets were used in all calculations: aug-cc-PVXZ (X = T, V, 5) sets were used for F, while aug-cc-PV(X+d)Z sets that include an additional tight d function were used for Cl.[16] For both of these basis sets, the shorthand notation AVXZ was adopted. In the case of ClF, complete basis set (CBS) limits were obtained through extrapolation using the following expression

$$E(x) = E_{CBS} + be^{-x} + ce^{-x^2} \tag{1}$$

where E_{CBS}, b, and c were obtained through a least-squares fit of the energies computed by various basis sets and x represents the basis set quality, for example, $x = 3$ for the AVTZ basis set.

Spectroscopic parameters were computed for ClF and ClF^+ via Dunham analysis,[17] which uses a least-squares fit around the minima of the potential energy curves; a sixth-order polynomial fit to eight energy values was used. For the size consistent RCCSD(T) method, the dissociation energies (D_e) were computed by subtracting the molecular energy from the energy of the fragments. For the non-size-consistent MRCI and MRCI+Q methods, D_e values were computed by moving the atoms to a separation of 100 Å and then subtracting the energy at the equilibrium bond length R_e. For diatomics, computed harmonic vibrational frequency ω_e values were used to make vibrational zero point energy (ZPE) corrections to bond energies (D_0) at the same level of theory used for calculating the equilibrium energies. For the ground states of ClF_2 to ClF_7, ZPE corrections were calculated at the BHLYP/AVTZ level (after reoptimizing the structures) using the Gaussian 03 package.[18]

For the diatomics, natural orbitals (NO) were obtained at the CASSCF level. The NOs were then transformed to approximate GVB orbitals[19] using the CI coefficients for the corresponding configuration:

$$\sigma_R = \sqrt{\frac{c_1'}{c_1' - c_2'}}\sigma_b + \sqrt{\frac{-c_2'}{c_1' - c_2'}}\sigma_a \qquad \sigma_L = \sqrt{\frac{c_1'}{c_1' - c_2'}}\sigma_b - \sqrt{\frac{-c_2'}{c_1' - c_2'}}\sigma_a \tag{2}$$

where σ_R and σ_L represent the approximate GVB orbitals, σ_b and σ_a are the bonding and antibonding natural orbitals, respectively, and c_1' and c_2' are the corresponding renormalized CI vector coefficients. The overlap (S_{RL}) between the GVB orbitals is computed as

$$S_{RL} = \frac{c_1' + c_2'}{c_1' - c_2'} \tag{3}$$

For large ClF_n species, RHF molecular orbitals are shown at the optimized RCCSD(T) geometries. Pipek−Mezey localization[20] was used to obtain localized molecular orbitals. The 2D contour cross sections of the orbitals were plotted using gnuplot (http://www.gnuplot.info).

III. An Overview of Bonding in ClF_n ($n = 1-7$)

The utility of a theoretical model depends on the understanding and predictions that it enables. The power of the recoupled pair bond model for describing molecules with hypervalent bonds is that it provides significant *a priori* insights into the structures, energetics, and low-lying excited states of these species. In this section, we enumerate the basic features of the model drawn from our studies[8] of SF_n and then apply that model to make predictions about the structure, energetics, and low-lying excited states of ClF_n species.

A. Guidelines for Understanding Hypervalent Bonding. On the basis of our studies of SF_n, we recognized the following trends in the bonding in XF_n species:

(A) Recoupled pair bonding makes two electrons available for bonding. We refer to these bonds collectively as the first and second recoupled pair bonds, although the second bond is essentially a conventional covalent bond.
  (1) The first recoupled pair bond is weaker than the analogous covalent bond because energy is expended to decouple the pair of electrons. The singly occupied orbital left over from the recoupling has substantial antibonding character, causing the first recoupled pair bond length to also be longer than the analogous covalent bond.
  (2) The second recoupled pair bond is formed with the leftover electron in the singly occupied antibonding orbital. It is much stronger than the first recoupled pair bond and is often stronger than the analogous covalent bond; the latter is due to a marked diminution in the antibonding character in the orbital involved in the second bond. In addition:
    (a) Forming a bond with the electron in the leftover orbital reduces the bond lengths in *both* recoupled pair bonds by decreasing the antibonding character of the orbital that the electron occupies.
    (b) If more than one singly occupied orbital is available after formation of the recoupled pair bond, bonding to the one left over from formation of the recoupled pair bond will be favored

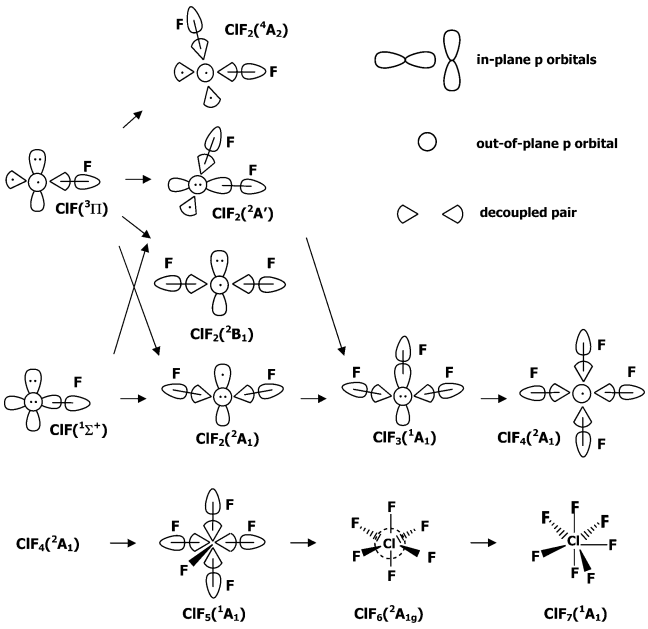

Figure 1. Coupling diagrams for the ClF_n ($n = 1-7$) series.

over normal covalent bonding to another singly occupied orbital.

(3) The two bonds resulting from the recoupled pair bond tend to be linear or quasilinear for electrons in orbitals with substantial p character, subject to minimizing electronic repulsion among all of the valence electrons.

(B) The bonding will rearrange if greater stability can be achieved: using both electrons from a recoupled pair is generally more energetically favorable than a combination of the first recoupled pair bond and a covalent bond. As a result, the atoms will rearrange, changing an existing covalent bond into a recoupled pair bond.

B. Applying the Guidelines to Make Predictions for ClF_n. Starting from Cl, we will now build up the possible states that can be formed by adding fluorine atoms one by one until each of the seven valence electrons of Cl are utilized in bonds. Coupling diagrams are shown in Figure 1. We will sometimes use the labels "equatorial" or "axial", which we associate with covalent and recoupled pair bonding, respectively (using the type of bond is preferable over using the geometric description, where the conventions can be confusing).

ClF. Diatomic ClF has low-lying states formed either by covalent or by recoupled pair bonding, with the former favored over the latter due to the energetic cost of decoupling a pair of electrons. Thus, the ground state ClF is $^1\Sigma^+$, where Cl and F form a normal covalent bond by coupling the electrons in the singly occupied Cl $3p_z$ and F $2p_z$ orbitals. However, if the Cl atom is rotated so that one of its $3p^2$ pairs is aligned with the internuclear axis, a $^3\Pi$ excited state would be formed via recoupled pair bonding. The second electron from the $3p^2$ pair in the $^3\Pi$ state will occupy an antibonding orbital with significant amplitude in the bond pair region. The triplet state will therefore have a much longer bond length than the singlet ground state as well as a much smaller bond energy.

ClF_2. Several possible states of ClF_2 can be formed by adding F to $ClF(^1\Sigma^+)$ and $ClF(^3\Pi)$. It is more straightforward to begin with the triplet state, where there are two unpaired electrons as well as a second $3p^2$ pair available for further bonding. As above, the states formed from the unpaired electrons are expected to be more stable (guideline A.1). Of the two options, it is energetically more favorable to form the second bond by forming a singlet coupled pair with the σ antibonding orbital left over from the recoupled pair bond. This would result in a $^2\Pi$ state (or $^2A_1$ and $^2B_1$ states if FClF is nonlinear and the bond lengths are equivalent) (guideline A.2.b). In these states, we expect a significant contraction in the bond lengths compared to $ClF(^3\Pi)$ (guideline A.2.a), a large bond angle (guideline A.3), and a larger bond energy than that of $ClF(^1\Sigma^+)$ (guideline A.2). Another state ($^2A_1$, if the bond lengths are equivalent, $^2A'$ otherwise) can be formed by covalently coupling the unpaired electron in the 2p orbital of F with the electron in the singly occupied π orbital of $ClF(^3\Pi)$. This state would be predicted to have a bond angle around 90°. Finally, a quartet state ($^4A_2$ or $^4A''$) would result if it is favorable for F to decouple the remaining $3p^2$ pair of Cl. The structure of this state would also be expected to have a bond angle around 90°, and it would lie significantly higher in energy than the doublet states.

If we start with $ClF(^1\Sigma^+)$, two of the doublet states can also be formed if F recouples a $3p^2$ pair. To reach ground state $ClF_2(^2A_1)$ via this pathway, the bonding rearranges per guideline B, which is more favorable than recoupling without bond rearrangement to form $ClF_2(^2A')$.

ClF_3. Closed-shell ClF_3 ($^1A_1$, if planar) would be formed by adding F to any of the doublet states of ClF_2. The pathway from the lowest state of ClF_2 is simple covalent bond formation, while the other pathway utilizes an electron in an orbital with antibonding character (the leftover orbital from the recoupled pair bond). Guideline A.2 thus accounts for the relative bond energies of these pathways. The ground state of ClF_3 has two types of bonds. The two axial bonds are the result of recoupled pair bonding, and the equatorial bond is a polar covalent bond. The axial bonds will be longer than the equatorial bond. In principle, F could also be added to ClF_2 ($^4A_2$) to form ClF_3 in a triplet state, but this state was not found to be stable in the present study.

ClF_4–ClF_7. To form ClF_4, the second pair of $3p^2$ lone pair electrons must be decoupled. Rearrangement is expected to occur to make two sets of recoupled pair bonds, leaving the unpaired electron available to form the covalent bond of ClF_5. The Cl $3s^2$ pair is the last to be decoupled to form ClF_6 and then ClF_7. However, crowding around Cl makes these species energetically unfavorable. The calculations show that normal recoupled pair bonding ceases with ClF_5, and ClF_6 and ClF_7 behave differently. This occurs in part because more energy is needed to decouple $3s^2$ pairs than $3p^2$ pairs, but the primary reason for the lower stability of ClF_6 and ClF_7 is steric in nature. More details will be discussed in section IV.

IV. Results of Calculations on ClF_n

Structures for the ground and low-lying excited electronic states of ClF_n species were optimized at the RCCSD(T) level with AVQZ basis sets for $n = 1-6$ and with AVTZ sets for $n = 7$. For ClF and ClF^+, MCSCF and MRCI calculations were also performed with sets as large as AV5Z. Figure 2 depicts the structures, formation pathways, and associated bond energies for ClF through ClF_6. The sequential bond energies (D_0) for atom-by-atom addition $ClF_{n-1} + F \rightarrow ClF_n$ are shown in Table 1 for ground state species. The results are also compared with the calculations reported by Van Huis et al.[21] As in that previous work, we find that ClF_7 is metastable with respect to $ClF_6 + F$.

The remainder of this section will describe each species in detail.

A. ClF. As shown in Figure 1, ClF has a covalently bonded $^1\Sigma^+$ ground state and a hypervalently bonded $^3\Pi$ excited state.

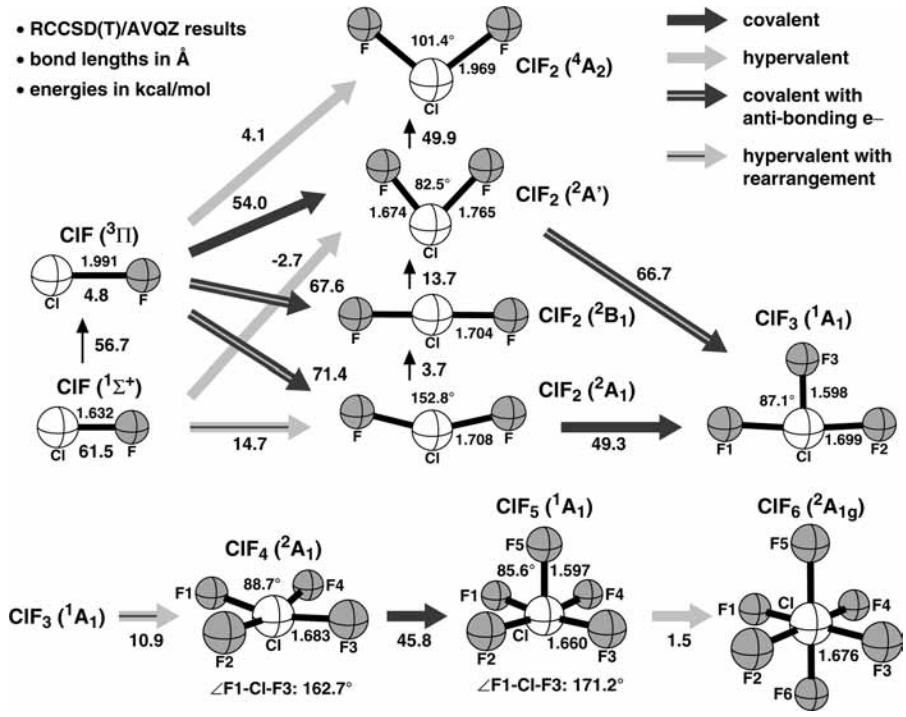

Figure 2. Formation pathways for ClF_n species. Equilibrium bond dissociation energies (D_e) are shown.

TABLE 1: Bond Energies (D_e) and Zero Point Energies (ZPEs) of ClF_n Species in Their Ground States

	D_e			ZPE[a]
bond[b]	RCCSD(T)/AVTZ	RCCSD(T)/AVQZ	ref 21[c]	BHLYP/DZP++
Cl−F	59.31	61.51	35.2	1.20
ClF−F	13.73	14.66	0.12	1.80
ClF_2−F	47.16	49.27	19.7	4.62
ClF_3−F	9.98	10.93	0.55	5.57
ClF_4−F	42.71	45.75	12.7	8.92
ClF_5−F	1.27	1.52	−11.56	8.12
ClF_6−F	−34.88	...	−57.2	13.01

[a] Current work. [b] D_e and ZPE are in kcal/mol. [c] BHLYP/DZP++ results.

To better quantify the differences between the two bonding processes, we computed the potential energy curves of the two states of ClF at various levels of theory. As shown in Figure 3, the ground state is bound at all levels of theory. Dynamic correlation accounts for about half of the 60 kcal/mol bond energy. For the $^3\Pi$ state, the CASSCF curve is repulsive. However, once dynamical correlation is taken into account (~20 kcal/mol at R_e), the interaction is sufficiently attractive to yield a weak bond of about 5 kcal/mol. At the MRCI+Q/CBS level, the bond energy of the $^3\Pi$ excited state is 8% of that of the ground state D_0. The equilibrium bond length (R_e) of the excited state is 0.45 Å longer than it is in the ground state at the same level of theory with the AV5Z basis set. Table 2 lists the structural parameters and the energies of the two states of ClF calculated at both the RCCSD(T) and MRCI+Q levels with various basis sets.

Further insight into the bonding in the two states can be gained by examining how the orbitals change as a function of internuclear separation during the bond formation process. Comparison between the orbitals in these states shows the fundamental difference between normal polar covalent and recoupled pair bonding. We will also compare the orbitals of the two states of ClF with those of the analogous covalent and hypervalent states of SF to gain additional understanding.

Figure 4 shows the valence NOs and GVB orbitals that are involved in the bond formation of ground state ClF. In both cases, the orbitals resemble the Cl $3p_z$ and F $2p_z$ orbitals at large Cl−F separation (delocalized bonding and antibonding linear combinations in the NO case, localized on the atoms in the GVB case). As the internuclear distance decreases, the bonding NO shows that electronic density shifts from Cl to F. At the equilibrium separation, the bonding orbital is mostly centered on F. The antibonding NO shows only limited delocalization from F to Cl. The GVB orbitals exhibit similar but slightly different trends. As the two atoms approach each other, the $7\sigma_L$ orbital delocalizes significantly toward the F atom, while the F orbital ($7\sigma_R$) shifts only slightly toward Cl. Although a significant amount of F $2p_z$ character is added to the $7\sigma_L$ orbital as the bond forms, it still has substantial Cl character. The overlap between the $7\sigma_L$ and $7\sigma_R$ orbitals in $ClF(^1\Sigma^+)$ is 0.71 at R_e. Compared to $SF(^2\Pi)$, the covalent bond in $ClF(^1\Sigma^+)$ is less polarized.

The bonding in $ClF(^3\Pi)$ is considerably weaker than that in the ground state. As shown in Figure 5, at large separation, the three orbitals of interest are the left and right lobe orbitals ($7\sigma_L$ and $7\sigma_R$) corresponding to the pair of Cl $3p_z$ electrons in a $3p_z-3d_{z2}$ hybrid orbital (but with only a small amount of $3d_{z2}$ character) and the F $2p_z$ orbital. As R decreases, there is a small amount of delocalization, from Cl to F and vice versa. It is most pronounced in the $7\sigma_L$ orbital, although even at R_e this orbital retains substantial Cl character. The GVB orbitals from $SF(^4\Sigma^-)$ at R_e are shown for comparison. To achieve the degree of recoupling that is evident in the hypervalent state of SF, it is necessary to reduce the Cl−F separation of $ClF(^3\Pi)$ well below its equilibrium separation (see orbitals at $R = 1.61$ Å in Figure 5). In summary, recoupling is very limited in $ClF(^3\Pi)$ at R_e. As a result, the Cl−F bond is very weak and the bond length is very large. Similar behavior was also observed in $OF(^4\Sigma^-)$,[22] which likewise has a small bond energy. The p^2 lone pairs in Cl and O are both more tightly bound than the S p^2 lone pair and are consequently much more difficult to recouple.

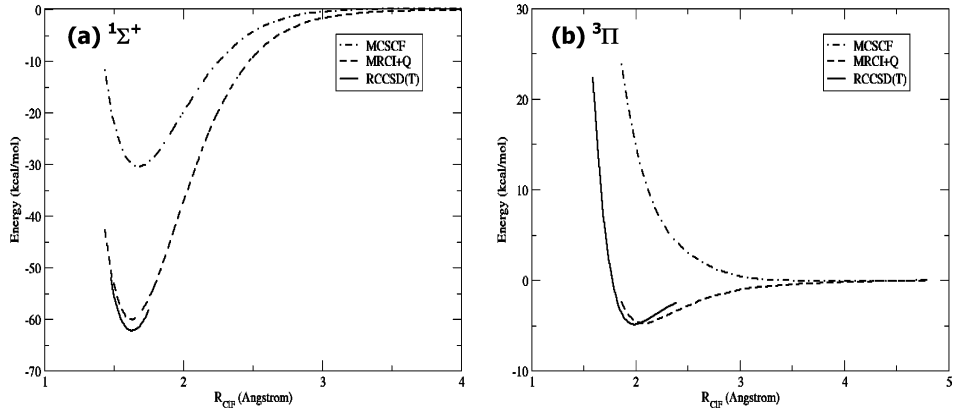

Figure 3. Potential energy curves for low-lying states of ClF calculated at the MCSCF, MRCI+Q, and RCCSD(T) levels with AV5Z basis sets: (a) $^1\Sigma^+$ ground state; (b) $^3\Pi$ excited state.

TABLE 2: Equilibrium Energies (E_h), Bond Lengths (R_{ClF}), Dissociation Energies (D_e and D_0), and Harmonic Vibrational Frequencies (ω_e) of ClF Computed via Dunham Analysis

property	basis set	ClF ($^1\Sigma^+$) RCCSD(T)	ClF ($^1\Sigma^+$) MRCI+Q	ClF ($^3\Pi$) RCCSD(T)	ClF ($^3\Pi$) MRCI+Q
energy (E_h)	AVTZ	−559.39983	−559.39062	−559.31241	−559.30612
	AVQZ	−559.44637	−559.43553	−559.35599	−559.34811
	AV5Z	−559.46165	−559.45004	−559.37031	−559.36168
	CBS	−559.47052	−559.45846	−559.37863	−559.36956
R_{ClF} (Å)	AVTZ	1.640	1.638	2.010	2.092
	AVQZ	1.632	1.631	1.991	2.075
	AV5Z	1.629	1.627	1.985	2.072
	expt.[a]	1.628			
D_e (kcal/mol)	AVTZ	59.31	57.53	4.45	4.57
	AVQZ	61.51	59.57	4.8	4.77
	AV5Z	62.21	60.18	4.9	4.73
	CBS	62.63	60.55	4.96	4.79
ω_e (cm^{-1})	AVTZ	774.0	782.3	305.3	240.20
	AVQZ	784.8	794.2	318.3	248.80
	AV5Z	788.2	797.8	321.2	250.00
	expt.[b]	784.1			
D_0 (kcal/mol)	AVTZ	58.20	56.41	4.04	4.24
	AVQZ	60.40	58.44	4.36	4.43
	AV5Z	61.09	59.03	4.45	4.38

[a] Reference 25. [b] Reference 26.

As in SF, it is instructive to determine the energy needed to remove electrons from various orbitals of both states of ClF. The optimized geometries of various ClF^+ states and the associated ionization potentials were calculated at the MRCI+Q level. Detailed results for a range of basis sets are shown in Tables 3 and 4, while the values obtained at the MRCI+Q/AV5Z level are shown with coupling diagrams in Figure 6. From the ground state of ClF, $ClF^+(^2\Pi)$ can be obtained by removing an electron from either of the doubly occupied π orbitals of $ClF(^1\Sigma^+)$. As expected, the ionization potential (IP) for this state, 12.56 eV, is roughly comparable to the IP for removing an electron from atomic Cl (12.967 eV).[23] From $ClF(^3\Pi)$, there are multiple ways to remove an electron to yield stable states of ClF^+. It is easiest to remove the electron from the 8σ antibonding orbital (IP = 10.19 eV), which also results in $ClF^+(^2\Pi)$. The bond length decreases by 0.53 Å, indicating the enormous impact of the singly occupied antibonding orbital on the structure of $ClF(^3\Pi)$. Alternatively, an electron can be removed from a π orbital, yielding states of $^4\Sigma^-$, $^2\Sigma^+$, and $^2\Delta$ symmetry. The most stable of these is $ClF^+(^4\Sigma^-)$, which has an IP of 12.51 eV and a bond length of 1.97 Å.

In summary, ClF, like SF, has a covalently bonded ground state and a low-lying hypervalently bonded excited state, but the latter is much more weakly bound than the corresponding $^4\Sigma^-$ state in SF. This behavior is consistent with the deeper energy of the $3p^2$ pairs in Cl over the one in S. Recoupling is less extensive in $ClF(^3\Pi)$. However, if the singly occupied orbital left over from recoupling can be utilized in a second bond, relieving the impact of its antibonding character, a much more stable species should be obtained. This is what is observed in ClF_2, which we discuss next.

B. ClF_2. As discussed in section III and depicted in Figure 2, there are four states of ClF_2 that can be formed by adding F to $ClF(^1\Sigma^+)$ or $ClF(^3\Pi)$. Table 5 lists the structural parameters and energies of the ClF_2 states calculated at the RCCSD(T) level with various basis sets. At least one of the lone pairs of 3p electrons on Cl must be decoupled to form ClF_2 from $ClF(^1\Sigma^+)$, but there is more than one way to form ClF_2 from $ClF(^3\Pi)$. The most stable state is $ClF_2(^2A_1)$, which uses both electrons from the recoupled pair and does not have a normal covalent Cl−F bond. The $^2B_1$ state is nearly degenerate with the $^2A_1$ state and has a linear geometry. In fact, the two states intersect at 180° for all Cl−F bond lengths and constitute a quasilinear−linear Renner−Teller system. The third state, $ClF_2(^2A')$, has both a covalent bond and a recoupled pair bond and is 17.4 kcal/mol less stable than the ground state. The $^4A_2$ state of ClF_2 lies nearly 50 kcal/mol higher than the 2A state in energy and is formed when both Cl 3p pairs are decoupled. We will discuss each of these states in turn and examine the pathways by which they can be formed.

Ground state $ClF_2(^2A_1)$ has a large bond angle of 152.8° and bond lengths of 1.708 Å, which is significantly shorter, 0.28 Å, than the bond length of $ClF(^3\Pi)$ and slightly longer (0.08 Å) than the bond length of $ClF(^1\Sigma^+)$. Two-dimensional (2D) cross sections of several NOs are depicted in Figure 7a. As expected, the singly occupied orbital ($9a_1$) resembles the 3p orbital of Cl. Breaking linearity allows this orbital and the one with strong Cl $3s^2$ character ($6a_1$) to minimize repulsion with the other electrons by displacing away on either side from the Cl nucleus. The doubly occupied, out-of-plane $4b_1$ orbital still very much resembles a Cl $3p^2$ lone pair orbital. $ClF_2(^2A_1)$ can be formed from $ClF(^3\Pi)$ with a bond energy of 71.4 kcal/mol, which is about 10 kcal/mol larger than the covalent bond energy of $ClF(^1\Sigma^+)$.

$ClF_2(^2A_1)$ can also be formed by recoupled pair bonding with $ClF(^1\Sigma^+)$, with a bond energy of 14.7 kcal/mol. While still very weak, it is about 10 kcal/mol larger than the bond energy of $ClF(^3\Pi)$ because both electrons from the Cl pair are being used. However, it is necessary to rearrange the bonding to allow this favorable structure. Initially, the F approaches from a direction

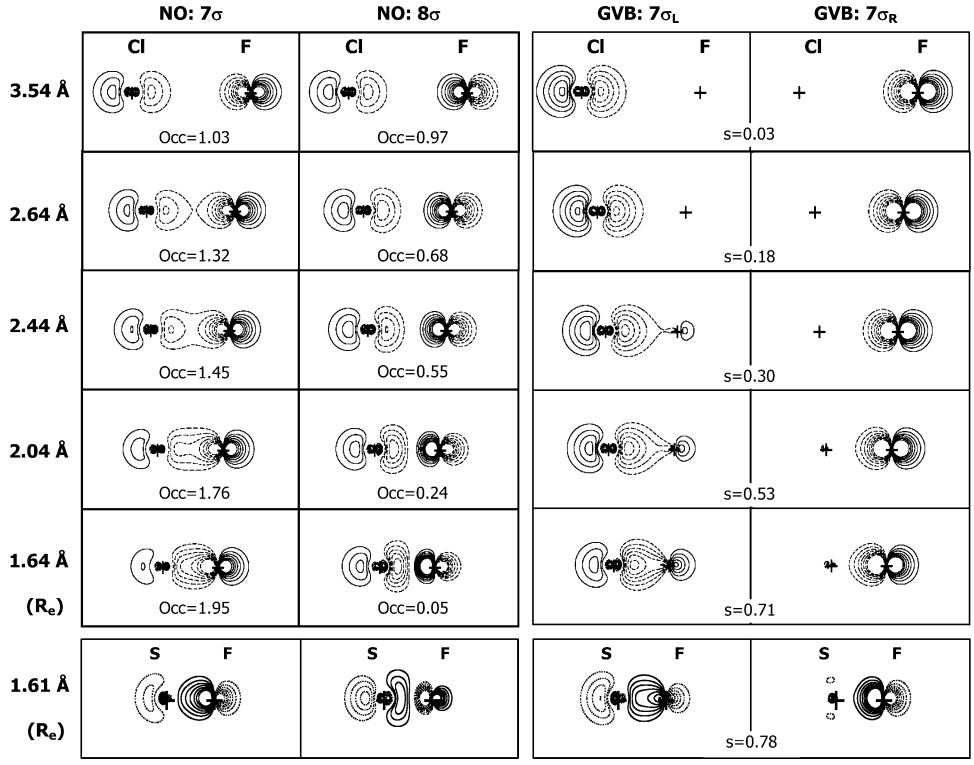

Figure 4. 2D sections of the natural orbitals (left two columns) and GVB orbitals (right two columns) during the formation of ground state ClF($^1\Sigma^+$) at various internuclear separations R. The corresponding orbitals for ground state SF($^2\Pi$) at R_e are shown for comparison in the bottom row. Positions of the nuclei are indicated with "+" symbols. Contours are 0.10, 0.15, 0.20, 0.25, and 0.30; positive amplitudes are represented by solid lines and negative amplitudes by dashed lines. The occupations (Occ) of each natural orbital and the overlaps (s) between the GVB orbitals are indicated.

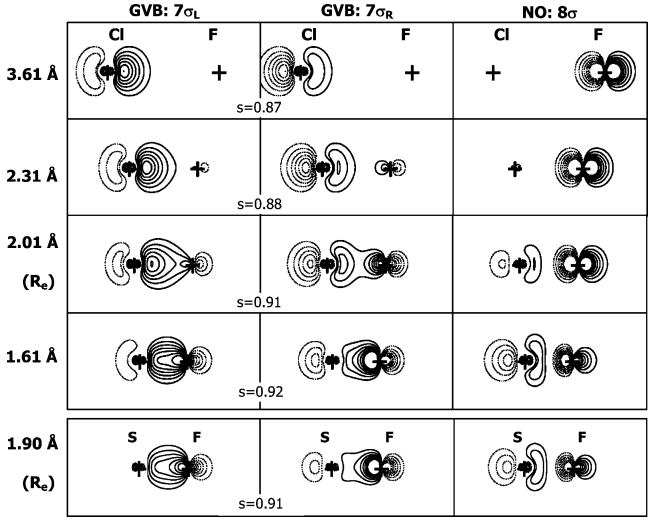

Figure 5. 2D sections of the GVB orbitals during the formation of excited state ClF($^3\Pi$) at various internuclear separations R. The corresponding orbitals for ground state SF($^4\Sigma^-$) at R_e are shown for comparison in the bottom row. See Figure 4 for notes about the symbols. The occupation of 8σ is 1.00 for all R.

roughly perpendicular to the ClF($^1\Sigma^+$) bond axis and then swings away as the bond forms. There is a transition state (with $^2A'$ symmetry) along this reaction pathway, but it lies about 1 kcal/mol below the reactant asymptote.

The $^2B_1$ state is linear. With its unpaired electron in an out-of-plane b_1 orbital, no additional stabilization is gained by bending as there was for the $^2A_1$ state; see Figure 7b. The $^2B_1$ state is just 3.7 kcal/mol above the ground state. If $ClF_2(^1A_1)$ is formed from either ground or excited state ClF, it will therefore be vibronically coupled to the $^2B_1$ state.

TABLE 3: Equilibrium Energies (E_h), Bond Lengths (R_{ClF}), Dissociation Energies (D_e and D_0), and Harmonic Vibrational Frequencies (ω_e) of ClF^+ Computed via Dunham Analysis

		$ClF^+(^2\Pi)$		$ClF^+(^4\Sigma)$	
property	basis sets	MRCI	MRCI+Q	MRCI	MRCI+Q
energy (E_h)	AVTZ	−558.89673	−558.93271	−558.81655	−558.85125
	AVQZ	−558.93638	−558.97488	−558.85284	−558.88979
	AV5Z	−558.94947	−558.98865	−558.86477	−558.90233
R_{ClF} (Å)	AVTZ	1.545	1.546	2.028	1.9927
	AVQZ	1.538	1.539	2.013	1.9779
	AV5Z	1.536	1.536	2.010	1.9745
D_e (kcal/mol)	AVTZ	60.59	63.616	10.37	12.52
	AVQZ	63.17	66.523	10.84	13.15
	AV5Z	64.00	67.438	11.13	13.59
ω_e (cm^{-1})	AVTZ	888.4	895.7	319.7	349.3
	AVQZ	899.9	907.5	331.5	361.6
	AV5Z	904.2	911.9	333.1	363.2
D_0 (kcal/mol)	AVTZ	59.33	62.33	9.92	12.01
	AVQZ	61.89	65.24	10.38	12.64
	AV5Z	62.70	66.14	10.65	13.08

The $^2A'$ state of ClF_2 can be formed from either ClF($^1\Sigma^+$) or ClF($^3\Pi$), though it is 2.7 kcal/mol endoergic for the former. This species has an acute bond angle of 82.5° and different bond lengths of 1.674 and 1.765 Å. The orbitals (Figure 7c) with Cl $3s^2$ and $3p^2$ character behave like the analogous orbitals in $ClF_2(^1A_1)$. The singly occupied 14a′ orbital has significant antibonding character and is mostly localized such that it is aligned with the longer of the two bonds. In spite of the antibonding character, both bonds are only modestly longer than the covalent bond in ClF($^1\Sigma^+$) by 0.042 and 0.133 Å, respectively. The addition of F to the π orbital in ClF($^3\Pi$) to form $ClF_2(^2A')$ results in a covalent bond, but the bond energy (54.0

TABLE 4: Ionization Potentials with and without Zero Point Energy Correction (IP_0 and IP_e) for Various States of $ClF \rightarrow ClF^+ + e^-$ at the MRCI+Q Level

	basis set	$ClF(^1\Sigma^+) \rightarrow ClF^+(^2\Pi) + e^-$	$ClF(^3\Pi) \rightarrow ClF^+(^2\Pi) + e^-$	$ClF(^3\Pi) \rightarrow ClF^+(^4\Sigma) + e^-$
IP_e[a]	AVTZ	12.46	10.16	12.38
	AVQZ	12.53	10.16	12.47
	AV5Z	12.56	10.16	12.50
IP_0[a]	AVTZ	12.47	10.20	12.38
	AVQZ	12.54	10.20	12.48
	AV5Z	12.56	10.19	12.51

[a] IPs are in eV.

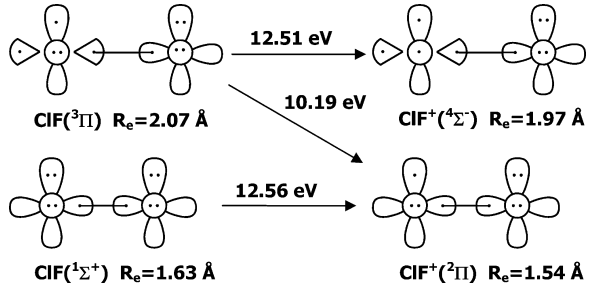

Figure 6. Coupling diagrams for various states of ClF^+ and ZPE-corrected ionization energies (MRCI+Q/AV5Z level).

kcal/mol) is 7.5 kcal/mol *smaller* than the bond energy of $ClF(^1\Sigma^+)$. This differs from the analogous situation of covalent bond formation in SF_2 and SF, where the $SF(^4\Sigma^-)$−F bond energy of $SF_2(^3A_2)$ is about 5 kcal/mol *larger* than the S−F bond energy of $SF(^2\Pi)$. This may be because the structures of these states are a compromise between the covalent and hypervalent bonds. Note, for example, that the lengths of the two bonds in $SF_2(^3A_2)$ were identical. $SF_2(^3A_2)$ appears to be better able to accommodate the antibonding orbital, since its bond length is only slightly larger than those found in purely covalent states. In $ClF_2(^2A')$, the longer bond length is still more than 0.1 Å longer than typical covalent bond lengths.

Finally, $ClF_2(^4A_2)$ is formed by decoupling the remaining Cl $3p^2$ pair in $ClF(^3\Pi)$. While this state is much less stable than the other two bound states, it is still weakly exoergic with respect to $ClF(^3\Pi) + F(^2P)$. The bond energy of 4.1 kcal/mol is very similar to that of $ClF(^3\Pi)$. The bond angle of $ClF_2(^4A_2)$ is 101.4°, and its bond length is very close to that of $ClF(^3\Pi)$. As shown in Figure 7d, two of its singly occupied orbitals ($9a_1$ and $6b_2$) have strong antibonding character. As in $ClF(^3\Pi)$, the bond length is too long to allow much delocalization.

C. ClF_3. Structural parameters and energies for ClF_3 calculated at the RCCSD(T) level with various basis sets are in Table 6. $ClF_3(^1A_1)$ has a planar structure with two axial bonds that are about 0.10 Å longer than the equatorial bond length of 1.597 Å. The F1−Cl−F3 bond angle is 87.1°, and the F1−Cl−F2 angle is 174.2°. The latter is about 20° larger than it is in $ClF_2(^2A_1)$. Two of the orbitals are shown in Figure 8a. The orbital with strong Cl $3s^2$ character ($8a_1$) only moves slightly away from the Cl atom, as it does in $ClF_2(^2A_1)$. This is significantly different from the behavior of the analogous orbitals of $SF_2(^3A_2)$ and $SF_2(^3B_1)$, which are displaced farther away from the S atom (see Figure 9 of ref 8). The Cl atom holds two electrons in the 3s orbital much tighter than S does. The doubly occupied orbital $2b_1$ holds the lone pair electrons of Cl and is perpendicular to the molecular plane. It provides the electrons for bonding in ClF_4 and ClF_5.

There are two pathways to form $ClF_3(^1A_1)$. Forming it from ground state ClF_2 is straightforward: the third F atom simply forms a covalent bond with the unpaired electron. The bond energy for this addition, 49.3 kcal/mol, is 12.2 kcal/mol less than the covalent bond energy of $ClF(^1\Sigma^+)$. $ClF_3(^1A_1)$ can also be formed by adding F to $ClF_2(^2A')$, which yields a bond energy of 66.7 kcal/mol; this is 5.2 kcal/mol larger than in the bond energy of $ClF(^1\Sigma^+)$ but 4.7 kcal/mol less than the energy for $ClF(^3\Pi) + F(^2P) \rightarrow ClF_2(^2A_1)$ bond formation.

D. ClF_4. Table 7 lists the structural parameters and energies for ClF_4−ClF_7 calculated at the RCCSD(T) level with various basis sets. The formation of $ClF_4(^2A_1)$ requires decoupling the second 3p lone pair of Cl in $ClF_3(^1A_1)$ (the $2b_1$ orbital shown in Figure 8a). This can be done by bringing the F atom from the direction perpendicular to the molecular plane. To avoid placing the resulting unpaired electron in an antibonding orbital, the bonding rearranges to the nearly planar structure shown in Figures 2 and 8b, which has two sets of recoupled pair bonds with equivalent bond lengths. As shown in the figure, the bond pairs are bent toward the singly occupied $13a_1$ orbital and away from the doubly occupied orbital with Cl $3s^2$ character. The bond energy is 10.9 kcal/mol, which is 6−7 kcal/mol larger than the hypervalent bond energies of $ClF(^3\Pi)$ and $ClF(^3\Pi) + F \rightarrow ClF_2(^4A_2)$ but 3.8 kcal/mol less than the bond energy of $ClF(^1\Sigma^+) + F \rightarrow ClF_2(^2A_1)$, where the bonding shifts to convert the covalent bond to a recoupled pair bond.

E. ClF_5. $ClF_5(^1A_1)$ is formed by coupling the available electron in $ClF_4(^2A_1)$ with the unpaired electron of a fifth F atom, yielding a normal covalent bond with an energy of 45.8 kcal/mol, only slightly smaller than what it is in ClF_3. The new bond has the same bond length as the covalent bond in $ClF_3(^1A_1)$, while the lengths of the equatorial bonds have decreased to 1.660 Å. To reduce electronic repulsion, the F1−Cl−F3 angle increases about 8° compared to what it is in $ClF_4(^2A_1)$. The orbital with Cl $3s^2$ character is shown in Figure 8c.

F. ClF_6 and ClF_7. To form ClF_6 and then ClF_7, the $3s^2$ electrons of Cl must be recoupled. This is much less favorable for Cl than it is for S, where the $3s^2$ electrons are used to form SF_5 and then SF_6. Various factors account for this. First, the $3s^2$ pair is much more tightly bound in Cl than in S, so comparably more energy must be expended to decouple the pair (as is well-known, all of the $n = 3$ IPs of Cl are higher than the corresponding ones of S,[23] indicating that it is harder to remove electrons from Cl than from S). As a result, $ClF_6(^2A_{1g})$ is only bound by 1.5 kcal/mol with respect to $ClF_5 + F$. In addition, with five existing Cl−F bonds, there is simply no good spatial location remaining for the antibonding orbital. As shown in Figure 8d, the singly occupied orbital is delocalized across all seven atoms of ClF_6. The ClF_6 bond length of 1.676 Å is longer than the equatorial bond lengths of ClF_5.

ClF_7 has an unusual D_{5h} structure, with five fluorine atoms crowded around the Cl in a plane. ClF_7 is not stable with respect to $ClF_6 + F$, with a bond energy that is endothermic by 34.9 kcal/mol at the RCCSD(T)/AVTZ level. Figure 8e shows that the two out-of-plane orbitals of ClF_7 are less polarized toward F than other ClF bonds. The $13a_1$ orbital indicates how the $3s^2$ orbital of Cl is involved in the bonding in ClF_7.

V. A Comparison of Hypervalency in SF_n and ClF_n

Some of the similarities and differences between the bonding in the SF_n and ClF_n series were noted in section IV. A more detailed comparison between the two series can provide more insights into the nature of hypervalent bonding. Figure 9 shows the potential energy curves for the covalently bonded ground states and the hypervalently bonded excited states of both SF and ClF. While the ground states have very similar bond lengths

TABLE 5: Energies, State Separations (T_e), and Structural Parameters for ClF_2 States at the RCCSD(T) Level

	$^2A_1$[a]		$^2B_1$		$^2A'$		$^4A_2$	
property	AVTZ	AVQZ	AVTZ	AVQZ	AVTZ	AVQZ	AVTZ	AVQZ
energy (E_h)	−659.04937	−659.12245	−659.04348	−659.11652	−659.02174	−659.09474	−658.94588	−659.01516
R_1 (Å)	1.716	1.708	1.711	1.704	1.768	1.765	1.990	1.969
R_2 (Å)					1.689	1.674		
θ	152.82	152.84	180.00	180.00	82.39	82.52	101.44	101.40
T_e (kcal/mol)			3.70	3.72	17.34	17.39	64.94	67.33

[a] Experimental bond angle: 140 ± 19° (ref 27); prior calculation [CCSD(T)/TZ2P]: $R_1 = 1.756$, $\theta = 151.8°$ (ref 28).

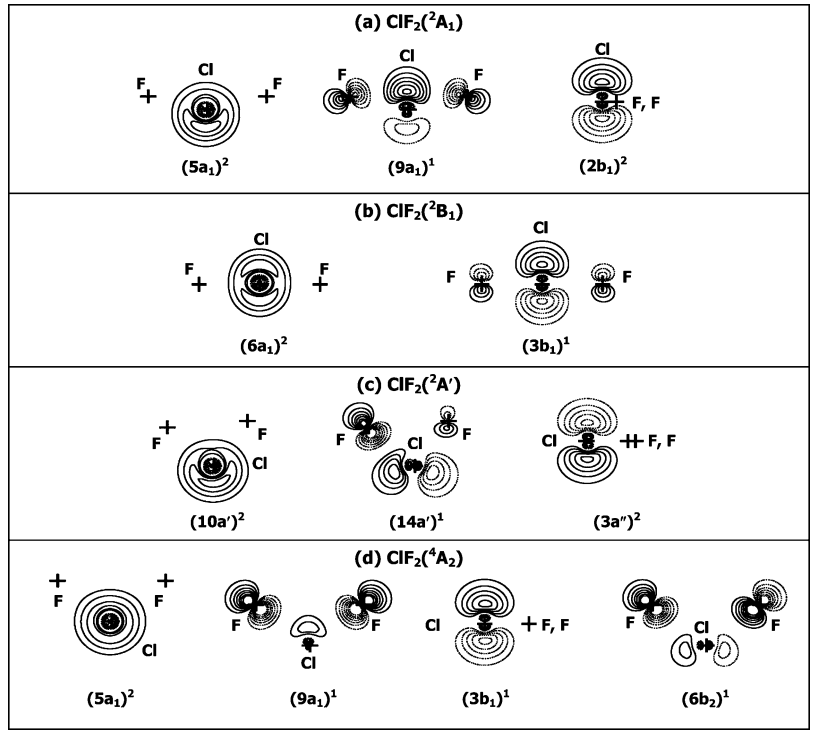

Figure 7. 2D sections of selected orbitals of various states of ClF_2: (a) $^2A_1$; (b) $^2B_1$; (c) $^2A'$; (d) $^4A_2$. The orbitals were calculated at the RHF level at the equilibrium geometries obtained from RCCSD(T)/AVQZ calculations. Other notations are the same as those in Figure 4.

TABLE 6: Energies and Structural Parameters of $ClF_3(^1A_1)$ Compared with Experiment and Prior Calculations

		RCCSD(T)			
property	expt[a]	AVTZ	AVQZ	AV5Z	ref 21[b]
energy (E_h)		−758.75218	−758.85368	−758.88793	
R_{ClF3} (Å)	1.598	1.605	1.598	1.595	1.598
R_{ClF1}(Å)	1.698	1.705	1.699	1.696	1.705
$\theta_{F1-Cl-F3}$	87.29	87.08	87.11	87.12	86.9

[a] Reference 29. [b] BHLYP/DZP^{++} results.

and bond energies that differ by about 20 kcal/mol, there is a much larger difference between the two excited states: hypervalent $SF(^4\Sigma^-)$ is much more strongly bound than $ClF(^3\Pi)$. As the orbitals demonstrated (Figure 5), recoupling is much less complete in ClF than it is in SF at R_e. The larger state separation of ClF (about 57 kcal/mol, versus about 45 kcal/mol for SF) is consistent with the expectation that the electrons in the lone pair orbitals are more tightly bound in Cl than in S.

The bond energies of the larger species continue this trend. Nevertheless, ClF_2 and larger hypercoordinated species are stable, particularly the closed-shell species with an odd number of F atoms. This is due to the much stronger second recoupled pair bond.

Oscillating large and small bond energies are observed in both the SF_n and ClF_n series. This oscillation occurs because of the energy required to decouple a lone pair, making the first recoupled pair bond much weaker than the second one, which is actually more strongly bonded than the analogous covalent bond in both SF_n and ClF_n species. The bond energies of the ClF_n family are smaller than the corresponding SF_n molecule, in part because of the additional repulsion due to the extra electron in Cl but mostly because Cl's electrons are more tightly bound and thus more difficult to recouple.

VI. Conclusion

As a consequence of our previous study of SF_n ($n = 1-6$) species, we proposed a new model for understanding hypervalency known as recoupled pair bonding. We found that the new model provided a rationale for understanding the structures and energies of the ground and low-lying excited states of the SF_n species. In this paper, we tested the model by (a) using the concepts to make predictions about the structures and energies of the ground and low-lying excited states of the ClF_n species ($n = 1-7$) and (b) performing high level *ab initio* calculations to determine the equilibrium energies and geometries of the ground and low-lying states of the molecules. Similar trends are found in both the SF_n and ClF_n series, and the differences are consistent with the difference between S and Cl at the atomic level (e.g., the relative energies of the 3s and 3p orbitals). Like SF,

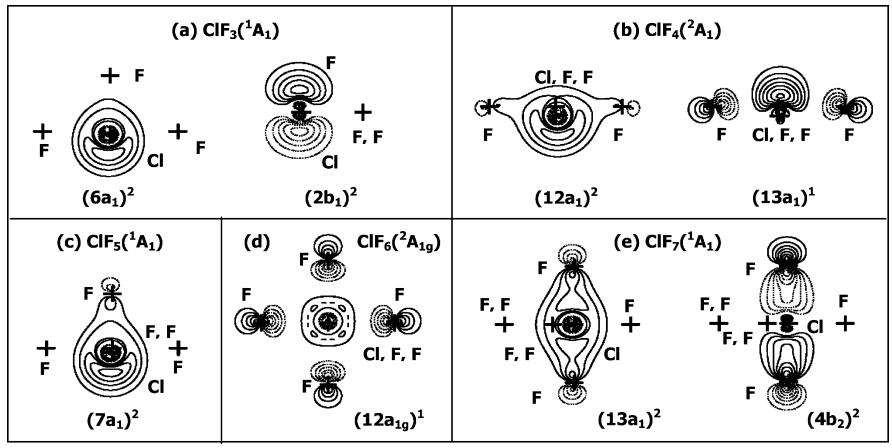

Figure 8. 2D sections of selected orbitals for ClF_n ($n = 3-7$): (a) $ClF_3(^1A_1)$; (b) $ClF_4(^2A_1)$; (c) $ClF_5(^1A_1)$; (d) $ClF_6(^2A_{1g})$; (e) $ClF_7(^1A_1)$. The orbitals are calculated at the RHF level at the equilibrium geometries obtained using RCCSD(T) methods with AVQZ basis sets except for ClF_7, which is calculated with the AVTZ basis set. Other notations are the same as those in Figure 4.

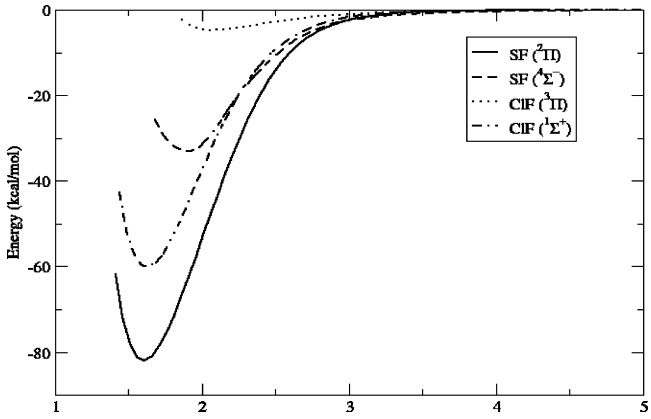

Figure 9. Comparisons between states of SF and ClF. Covalently bonded states are $SF(^2\Pi)$ and $ClF(^1\Sigma^+)$; hypervalently bonded states are $SF(^4\Sigma^-)$ and $ClF(^3\Pi)$. The potential energy surfaces are calculated using the RCCSD(T) method with the AV5Z basis set.

TABLE 7: Energies and Structural Parameters for Ground States of ClF_4 through ClF_7 Compared with Experiment and Prior Calculations

		RCCSD(T)		
species	property	AVTZ	AVQZ	ref 21[a]
$ClF_4(^2A_1)$	energy (E_h)	−858.39575	−858.52382	
	R_e	1.689	1.683	1.693
	$\theta_{F1-Cl-F3}$	162.56	162.65	163.00
$ClF_5(^1A_1)^b$	energy (E_h)	−958.09307	−958.24945	
	R_{ClF5} (Å)	1.604	1.597	1.605
	R_{ClF1} (Å)	1.666	1.660	1.666
	$\theta_{F1-Cl-F5}$	85.58	85.60	85.50
$ClF_6(^2A_{1g})$	energy (E_h)	−1057.72275	−1057.90459	
	R_e (Å)	1.681	1.676	1.681
$ClF_7(^1A_1)$	energy (E_h)	−1157.29484		
	R_{ClF5} (Å)	1.571978		1.578
	R_{ClF1} (Å)	1.752		1.741

[a] BHLYP/DZP^{++} results. [b] Experimental values: $R_{ClF5} = 1.571$ Å, $R_{ClF1} = 1.669$ Å data (ref 30).

hypervalent behavior begins with diatomic ClF, not with the larger hypercoordinated species.

Even though the studies on SF_n and ClF_n have demonstrated the value of the recoupled pair bonding model, many other systems need to be studied to better assess the robustness of this model. For example, studies are needed of the PF_n series (already underway) as well as various combinations of P, S, Cl, and F with other ligands such as monovalent H, Cl, and OH (studies of the first two are also underway) and divalent O. Recoupled pair bonding is also likely to affect the reactivity of hypervalent species, for example, by opening new reaction pathways. One only needs to note the unusual pathway for the reaction

$$SF_2 + SF_2 \rightarrow FS - SF_3$$

to appreciate the unusual chemistry possible with hypervalent species.[24] We have begun to explore the $ClF + F_2 \rightarrow ClF_3$ reaction.

Acknowledgment. Support for this work was provided by funding from the Distinguished Chair for Research Excellence in Chemistry at the University of Illinois at Urbana—Champaign.

References and Notes

(1) Musher, J. I. *Angew. Chem., Int. Ed.* **1969**, *8*, 54.
(2) Schleyer, P. v. R. *Chem. Eng. News* **1984**, *62*, 4.
(3) (a) Pitzer, K. S. *Science* **1963**, *139*, 414. (b) Brown, R. D.; Peel, J. B. *Aust. J. Chem.* **1968**, *21*, 2605. (c) Kutzelnigg, W. *Angew. Chem., Int. Ed.* **1984**, *23*, 272. (d) Reed, A. E.; Weinhold, F. *J. Am. Chem. Soc.* **1986**, *108*, 3586. (e) Reed, A. E.; Schleyer, P. v. R. *J. Am. Chem. Soc.* **1990**, *112*, 1434. (f) Magnusson, E. *J. Am. Chem. Soc.* **1990**, *112*, 7940. (g) Pacchioni, G.; Bagus, P. S. *Inorg. Chem.* **1992**, *31*, 4391. (h) Glendening, E. D.; Badenhoop, J. K.; Weinhold, F. *J. Comput. Chem.* **1998**, *19*, 628. Gilheany, D. G. *Chem. Rev.* **1994**, *94*, 1339. Cooper, D. L.; Cunningham, T. P.; Gerratt, J.; Karadakov, P. B.; Raimondi, M. *J. Am. Chem. Soc.* **1994**, *116*, 4414. Gillbro, T.; William, F. *J. Am. Chem. Soc.* **1974**, *96*, 5032.
(4) Jensen, W. B. *J. Chem. Educ.* **2006**, *83*, 1751.
(5) Rundle, R. E. *J. Am. Chem. Soc.* **1947**, *69*, 1327.
(6) Pimentel, G. C. *J. Chem. Phys.* **1951**, *19*, 446.
(7) (a) Harcourt, R. D. *J. Chem. Educ.* **1968**, *45*, 779. (b) Harcourt, R. D. *Int. J. Quantum Chem.* **1996**, *60*, 553. (c) Curnow, O. J. *J. Chem. Educ.* **1998**, *75*, 910. (d) Gillespie, R. J.; Robinson, E. A. *Inorg. Chem.* **1995**, *34*, 978. (e) Noury, S.; Silvi, B.; Gillespie, R. J. *Inorg. Chem.* **2002**, *41*, 2164. (f) Gillespie, R. J.; Silvi, B. *Coord. Chem. Rev.* **2002**, *233−234*, 53. (g) Cioslowski, J.; Surján, P. R. *J. Mol. Struct. Theochem.* **1992**, *87*, 9. (h) Cioslowski, J.; Mixon, S. T. *Inorg. Chem.* **1993**, *32*, 3209. (i) Ponec, R.; Duben, A. J. *J. Comput. Chem.* **1999**, *20*, 760. (j) Ponec, R.; Gironés, X. *J. Phys. Chem. A* **2002**, *106*, 9506.
(8) Woon, D. E.; Dunning, T. H., Jr. *J. Phys. Chem. A* **2009**, *133*, 7915.
(9) Kiang, T.; Zare, R. N. *J. Am. Chem. Soc.* **1980**, *102*, 4024.
(10) When recoupled pair bonding occurs in C, the antibonding orbital does not overlap strongly with the bond pair; the recoupled pair bond in $CH(^4\Sigma^-)$ is almost as strong as the covalent bond in $CH(^2\Pi)$, and the equilibrium bond lengths of the two states are nearly the same.
(11) Werner, H.-J.; Knowles, P. J.; Amos, R. D.; Bernhardsson, A.; Berning, A.; Celani, P.; Cooper, D. L.; Deegan, M. J. O.; Dobbyn, A. J.; Eckert, F.; Hampel, C.; Hetzer, G.; Korona, T.; Lindh, R.; Lloyd, A. W.;

McNicholas, S. J.; Manby, F. R.; Meyer, W.; Mura, M. E.; Nicklass, A.; Palmieri, P.; Pitzer, R.; Rauhut, G.; Schütz, M.; Schumann, U.; Stoll, H.; Stone, A. J.; Tarroni, R.; Thorsteinsson, T. *Molpro*, version 2002.6; University College Cardiff Consultants Ltd.: Cardiff, U.K., 2004.

(12) (a) Purvis, G. D., III; Bartlett, R. J. *J. Chem. Phys.* **1982**, *76*, 1910. (b) Raghavachari, K.; Trucks, G. W.; Pople, J. A.; Head-Gordon, M. *Chem. Phys. Lett.* **1989**, *157*, 479. (c) Knowles, P. J.; Hampel, C.; Werner, H.-J. *J. Chem. Phys.* **1993**, *99*, 5219. (d) Watts, J. D.; Gauss, J.; Bartlett, R. J. *J. Chem. Phys.* **1993**, *98*, 8718.

(13) (a) Werner, H.-J.; Knowles, P. J. *J. Chem. Phys.* **1985**, *82*, 5053. (b) Knowles, P. J.; Werner, H.-J. *Chem. Phys. Lett.* **1985**, *115*, 259.

(14) (a) Werner, H.-J.; Knowles, P. J. *J. Chem. Phys.* **1988**, *89*, 5803. (b) Knowles, P. J.; Werner, H.-J. *Chem. Phys. Lett.* **1988**, *145*, 514.

(15) (a) Langhoff, S. R.; Davidson, E. R. *Int. J. Quantum Chem.* **1974**, *8*, 61. (b) Davidson, E. R.; Silver, D. W. *Chem. Phys. Lett.* **1977**, *52*, 403.

(16) (a) Dunning, T. H., Jr. *J. Chem. Phys.* **1989**, *90*, 1007. (b) Kendall, R. A.; Dunning, T. H., Jr.; Harrison, R. J. *J. Chem. Phys.* **1992**, *96*, 6796. (c) Woon, D. E.; Dunning, T. H., Jr. *J. Chem. Phys.* **1993**, *98*, 1358. (d) Dunning, T. H., Jr.; Peterson, K. A.; Wilson, A. K. *J. Chem. Phys.* **2001**, *114*, 9244.

(17) Dunham, J. L. *Phys. Rev.* **1932**, *41*, 721.

(18) Frisch, M. J.; Trucks, G. W.; Schlegel, H. B.; Scuseria, G. E.; Robb, M. A.; Cheeseman, J. R.; Montgomery, J. A., Jr.; Vreven, T.; Kudin, K. N.; Burant, J. C.; Millam, J. M.; Iyengar, S. S.; Tomasi, J.; Barone, V.; Mennucci, B.; Cossi, M.; Scalmani, G.; Rega, N.; Petersson, G. A.; Nakatsuji, H.; Hada, M.; Ehara, M.; Toyota, K.; Fukuda, R.; Hasegawa, J.; Ishida, M.; Nakajima, T.; Honda, Y.; Kitao, O.; Nakai, H.; Klene, M.; Li, X.; Knox, J. E.; Hratchian, H. P.; Cross, J. B.; Bakken, V.; Adamo, C.; Jaramillo, J.; Gomperts, R.; Stratmann, R. E.; Yazyev, O.; Austin, A. J.; Cammi, R.; Pomelli, C.; Ochterski, J. W.; Ayala, P. Y.; Morokuma, K.; Voth, G. A.; Salvador, P.; Dannenberg, J. J.; Zakrzewski, V. G.; Dapprich, S.; Daniels, A. D.; Strain, M. C.; Farkas, O.; Malick, D. K.; Rabuck, A. D.; Raghavachari, K.; Foresman, J. B.; Ortiz, J. V.; Cui, Q.; Baboul, A. G.; Clifford, S.; Cioslowski, J.; Stefanov, B. B.; Liu, G.; Liashenko, A.; Piskorz, P.; Komaromi, I.; Martin, R. L.; Fox, D. J.; Keith, T.; Al-Laham, M. A.; Peng, C. Y.; Nanayakkara, A.; Challacombe, M.; Gill, P. M. W.; Johnson, B.; Chen, W.; Wong, M. W.; Gonzalez, C.; Pople, J. A. *Gaussian 03*, revision C.02; Gaussian, Inc.: Wallingford, CT, 2004.

(19) Goddard, W. A., III; Dunning, T. H., Jr.; Hunt, W. J.; Hay, P. J. *Acc. Chem. Res.* **1973**, *6*, 368.

(20) Pipek, J.; Mezey, P. G. *J. Chem. Phys.* **1989**, *90*, 4916.

(21) Van Huis, T. J.; Galbraith, J. M.; Schaefer, H. F., III. *Mol. Phys.* **1996**, *89*, 607.

(22) Woon, D. E.; Dunning, T. H. *Mol. Phys.* **2009**, *107*, 991.

(23) Lide, D. R., Ed. *Handbook of Chemistry and Physics*, 89th ed.; CRC Press: Cleveland, OH, 2008; pp 10−203.

(24) Steudel, Y.; Steudel, R.; Wong, M. W.; Lentz, D. *Eur. J. Inorg. Chem.* **2001**, *2001*, 2543.

(25) Huber, K. P.; Herzberg, G. *Molecular Spectra and Molecular Structure. Constants of Diatomic Molecules*; 1st ed.; Van Nostrand-Reinhold: New York, 1979.

(26) Krasnov, K. S.; Philippenko, N. V.; Bobkova, V. A.; Lebedeva, N. L.; Morozov, E. V.; Ustinova, T. I.; Romanova, G. A. *Molecular Constants of Inorganic Compounds. Handbook*, 2nd ed.; Khimia: Leningrad, Russia, 1979.

(27) Mamantov, G.; Vickroy, D.; Vasini, E. J.; Maekawa, T.; Moulton, M. C. *Inorg. Nucl. Chem. Lett.* **1970**, *6*, 701.

(28) Galbraith, J. M.; Vacek, G.; Schaefer, H. F., III. *J. Chem. Phys.* **1993**, *98*, 8051.

(29) Smith, D. F. *J. Chem. Phys.* **1953**, *21*, 609.

(30) Begun, G. M.; Fletcher, W. H.; Smith, D. F. *J. Chem. Phys.* **1965**, *42*, 2236.

JP905064V